

# Effective fields approach for the Maxwell's equations for a mechano-driven media system that moves without solid translation

Zhong Lin Wang\*

Beijing Institute of Nanoenergy and Nanosystems, Chinese Academy of Sciences, Beijing 101400, P. R. China

\*\* e-mail: [zlwang@gatech.edu](mailto:zlwang@gatech.edu)

## Abstract

For engineering electromagnetism, one of a typical case is that a medium/object rotates possibly with a deformable time-dependent shape. The electrodynamic behavior of such a system is governed by the Maxwell's equations for a mechano-driven media system (MEs-f-MDMS). Here, by defining the effective electric and magnetic fields, the MEs-f-MDMS reduces to the standard form of the Maxwell's equations (MEs) if the medium has no translational motion. This means that the accelerated motion of a medium is a source for generating electromagnetic wave, while the propagation of the waves in the system follows the classical MEs. Therefore, the standard methods for solving the MEs can be adequately applied. We first present the theoretical derivation, then we will present the solutions of the MEs-f-MDMS in both time- and frequency space. Secondly, the shortcomings in classical approach regarding to the calculation of electromagnetic radiation from a rotating medium is analyzed. Thirdly, the theory about the impact of medium rotation on reflection and transmission of a plane wave at an interface is considered. Fourth, the theory for quantifying the output of triboelectric nanogenerator is given. Fifth, since the effective fields warrant the covariance of the MEs, the Lorentz transformation can be introduced for extrapolating the effective medium theory to a case there is a translation motion of the system. Finally, recent progresses about the experimental proofs in supporting the MEs-f-MDMS are covered.

## 1. Introduction

The conventional method for analyzing the electrodynamics of a moving medium system in inertial reference frames relies on the Lorentz transformation, which assumes the covariance of Maxwell's equations (MEs) [1,2,3]. This approach has proven highly successful in describing the electromagnetism of moving point charges in free space, as the invariance of the speed of light is strictly maintained in such a vacuum. It is a

standard framework in theoretical physics because the MEs hold precisely in inertial frames where the media are stationary relative to the origin of the chosen reference frame [4,5,6]. However, when dealing with accelerated motion, the moving reference frame becomes non-inertial, implying the presence of an external force acting on the system. In such cases, the absolute covariance of the MEs may no longer be guaranteed.

In practical applications, we often encounter problems involving rotating media or objects, such as the rotors in power generators. These systems involve complex coupling among electric, magnetic, and mechanical forces. Due to the dispersive nature of the medium, the speed of light varies with frequency, making it necessary to account for the dielectric properties of the media in calculations. Additionally, the presence of boundaries and multiple media further complicates the theory, rendering electromagnetic theories developed for free-space scenarios, such as relativity, less directly applicable to real-world situations. Recently, by starting from fundamental physical principles and adopting a systematic approach, we have derived the Maxwell's equations for a mechano-driven media system (MEs-f-MDMS) under the low-speed approximation ( $v \ll c$ ) [7,8,9,10]. This formulation is valid in Galilean space and time, making it suitable for systems with low-speed motion [11,12]. Previously, we introduced general methods for solving the MEs-f-MDMS by combining Green's function and perturbation theory. These approaches are applicable to cases where the medium exhibits both translational and rotational motion. However, due to the complexity of the problem, the final solutions can only be obtained through perturbation theory.

In this paper, we examine a scenario where the medium has no translational motion but rotates relative to the origin of the observation reference frame. By defining effective electric and magnetic fields, the MEs-f-MDMS can be simplified to the standard form of Maxwell's equations (MEs). This allows the application of established methods from the literature for solving the MEs. Our findings reveal that the motion of the medium introduces a local correction to the observed electric and magnetic fields, while the interaction of these effective fields with the system adheres to the standard MEs. We will explore the solutions to this system and discuss their practical implications in various engineering applications.

## 2. The Maxwell's equations for a mechano-driven system

For a system that is composed of moving media/objects, the electromagnetic behavior of the system is described in the Lab frame ( $S$  frame) in which the observer is located in, and a moving medium is present in the space that is traveling with a reference center  $S'$  associated with the medium at  $\mathbf{v}(t)$ . The electromagnetic behavior inside the moving medium is described by the MEs-f-MDMS equations, which are given by [8]:

$$\nabla \cdot \mathbf{D} = \rho \quad (1a)$$

$$\nabla \cdot \mathbf{B} = 0 \quad (1b)$$

$$\nabla \times (\mathbf{E} + \mathbf{v}_r \times \mathbf{B}) = -\frac{\partial}{\partial t} \mathbf{B} \quad (1c)$$

$$\nabla \times (\mathbf{H} - \mathbf{v}_r \times \mathbf{D}) = \mathbf{J} + \rho \mathbf{v} + \frac{\partial}{\partial t} \mathbf{D} \quad (1d)$$

where the total moving velocity is:

$$\mathbf{v}_t = \mathbf{v}(t) + \mathbf{v}_r(\mathbf{r}, t) \quad (2)$$

where  $\mathbf{v}$  is the translation speed of the origin of the reference frame  $S'$  that may be selected as the mass or geometrical center of the object, which is only time-dependent; and  $\mathbf{v}_r$  is the relative moving velocity of the medium with respect to the reference frame  $S'$ , which is space- and time-dependent, and can be simply referred to as “rotation speed”. The space-dependent nature of the problem implies that the object can exhibit time-varying shapes, sizes, and boundaries. As indicated by Eqs. (1a-d), the motion of a medium serves as a source for generating electromagnetic waves. This is a critical insight that will be further elaborated in the text. General methods for solving Eqs. (1a-d) have been previously presented [13].

The MEs-f-MDMS involve four variables:  $\mathbf{E}$ ,  $\mathbf{D}$ ,  $\mathbf{B}$  and  $\mathbf{H}$ , which are interdependent. In the case of a uniformly moving medium, the relationships among these variables are defined by the constitutive relations. For a medium undergoing accelerated motion, the constitutive relations derived for uniform motion can be extended to the low-speed approximation case by substituting the velocity  $\mathbf{v}$  with the time-dependent velocity  $\mathbf{v}_t$  [14]:

$$\mathbf{D} \approx \varepsilon \mathbf{E} + \varepsilon \mu \mathbf{v}_t \times \mathbf{H} \quad (3a)$$

$$\mathbf{B} \approx \mu \mathbf{H} - \varepsilon \mu \mathbf{v}_t \times \mathbf{E} \quad (3b)$$

Substituting Eqs. (3a-b) into Eqs. (1a-d), and ignore the second order terms of velocity, we have:

$$\varepsilon \nabla \cdot (\mathbf{E} + \mu \mathbf{v}_t \times \mathbf{H}) = \rho \quad (4a)$$

$$\mu \nabla \cdot (\mathbf{H} - \varepsilon \mathbf{v}_t \times \mathbf{E}) = 0 \quad (4b)$$

$$\nabla \times (\mathbf{E} + \mu \mathbf{v}_r \times \mathbf{H}) \approx -\mu \frac{\partial}{\partial t} (\mathbf{H} - \varepsilon \mathbf{v}_t \times \mathbf{E}) \quad (4c)$$

$$\nabla \times (\mathbf{H} - \varepsilon \mathbf{v}_r \times \mathbf{E}) \approx \mathbf{J} + \rho \mathbf{v} + \varepsilon \frac{\partial}{\partial t} (\mathbf{E} + \mu \mathbf{v}_t \times \mathbf{H}) \quad (4d)$$

These four equations are the fundamentals of the MEs-f-MDMS equations, which will be used in following sections.

### 3. Special case: no translation motion

#### 3.1 General equations

In practical engineering, there are many cases that has no translation motion but rotation motion of the object. In this case, we have  $\mathbf{v} = 0$ , so that  $\mathbf{v}_t(\mathbf{r}, t) = \mathbf{v}_r(\mathbf{r}, t)$ . For the case where the system not only rotates around the origin but also undergoes expansion or contraction in its surface, volume, and boundaries, Eqs. (4a-b) simplify to:

$$\varepsilon \nabla \cdot \mathbf{E}_{eff} = \rho \quad (5a)$$

$$\mu \nabla \cdot \mathbf{H}_{eff} = 0 \quad (5b)$$

$$\nabla \times \mathbf{E}_{eff} \approx -\mu \frac{\partial}{\partial t} \mathbf{H}_{eff} \quad (5c)$$

$$\nabla \times \mathbf{H}_{eff} \approx \mathbf{J} + \varepsilon \frac{\partial}{\partial t} \mathbf{E}_{eff} \quad (5d)$$

where the effective fields are defined by:

$$\mathbf{E}_{eff} = \mathbf{E} + \mu \mathbf{v}_r \times \mathbf{H}, \quad (6a)$$

$$\mathbf{H}_{eff} = \mathbf{H} - \varepsilon \mathbf{v}_r \times \mathbf{E}. \quad (6b)$$

Equations (5a-d) are identical to the classical Maxwell equations except that the electric field  $\mathbf{E}$  and magnetic field  $\mathbf{H}$  are replaced by the effective fields  $\mathbf{E}_{eff}$  and  $\mathbf{H}_{eff}$ , respectively. In Eq. (6a), the second term on the right-hand side represents the Lorentz force. Similarly, in Eq. (6b), the second term accounts for the contribution of the local electric field to the local magnetic field due to the motion of the medium. The physical interpretation of Eqs. (6a-b) is as follows: the motion of a medium acts as a source for generating electromagnetic fields; the movement of a medium within a magnetic field introduces an additional component to the electric field; and the motion of a medium within an electric field generates an additional term in the magnetic field. The propagation, scattering, and reflection of these effective fields adhere to the classical Maxwell equations, just as they would in the absence of medium motion.

The corresponding boundary conditions for the total solution are:

$$(\varepsilon_a \mathbf{E}_{eff,a} - \varepsilon_b \mathbf{E}_{eff,b}) \cdot \mathbf{n} = \sigma \quad (7a)$$

$$(\mu_a \mathbf{H}_{eff,a} - \mu_b \mathbf{H}_{eff,b}) \cdot \mathbf{n} = 0 \quad (7b)$$

$$\mathbf{n} \times (\mathbf{E}_{eff,a} - \mathbf{E}_{eff,b}) \approx 0 \quad (7c)$$

$$\mathbf{n} \times (\mathbf{H}_{eff,a} - \mathbf{H}_{eff,b}) \approx \mathbf{K}_s + \sigma \mathbf{v}_s \quad (7d)$$

where subscripts a and b refer to the two media that form the boundary,  $\mathbf{n}$  is the surface normal direction,  $\mathbf{K}_s$  is the surface current density,  $\sigma$  is the surface free charge density, and  $\mathbf{v}_s$  is the moving velocity of the media in parallel to the boundary.

Using  $\mathbf{v}_r \times \mathbf{E}_{eff}$  and  $\mathbf{v}_r \cdot \mathbf{H}_{eff}$  type of calculations as applied to Eqs. (6a-b), we can derive the  $\mathbf{E}$  and  $\mathbf{H}$  from  $\mathbf{E}_{eff}$  and  $\mathbf{H}_{eff}$  under low speed approximation  $\mu \varepsilon v_r^2 \ll 1$ :

$$\mathbf{E} \approx \mathbf{E}_{eff} - \mu \mathbf{v}_r \times \mathbf{H}_{eff} - \mu \varepsilon \mathbf{v}_r (\mathbf{v}_r \cdot \mathbf{E}_{eff}), \quad (8a)$$

$$\mathbf{H} \approx \mathbf{H}_{eff} + \varepsilon \mathbf{v}_r \times \mathbf{E}_{eff} - \mu \varepsilon \mathbf{v}_r (\mathbf{v}_r \cdot \mathbf{H}_{eff}). \quad (8b)$$

This means that the effective fields ( $\mathbf{E}_{eff}$  and  $\mathbf{H}_{eff}$ ) can be received from the standard MEs, and the true electric and magnetic fields ( $\mathbf{E}$  and  $\mathbf{H}$ ) can be derived following Eqs. (8a-b). Figure 1 shows the relationship between the effective fields derived inside the medium with that in free-space. The two sets of equations are identical except the definition of the fields are different owing to the rotation of the medium.

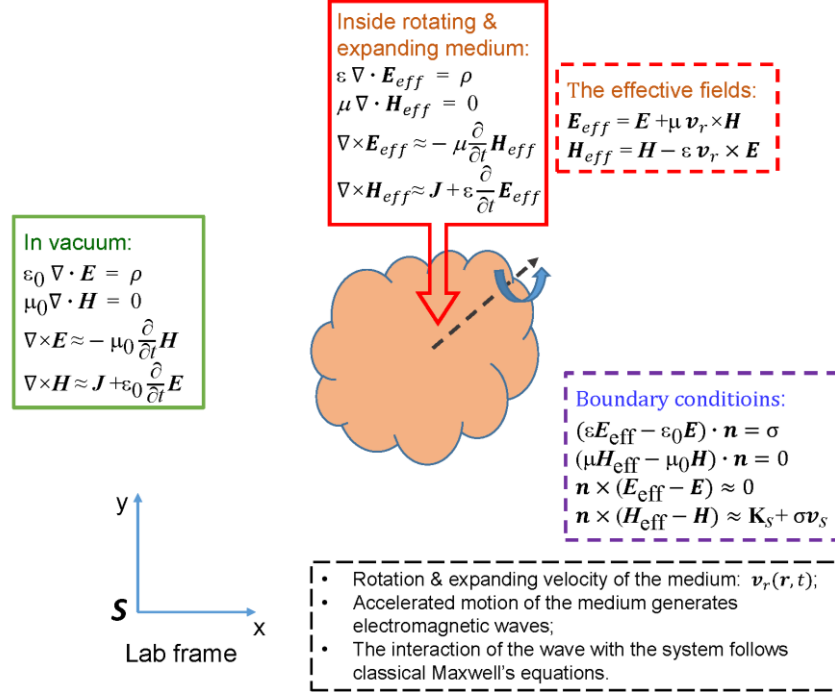


Figure 1. Schematic and governing equation for describing the electrodynamics of a medium that is rotating possibly with volume/surface expansion/contraction. The governing equations are listed and the associated boundary conditions are given.

### 3.2 Conservation of energy

The conservation of energy in the mechano-electric-magnetic coupling system is considered. The energy conservation process in this mechano-electric-magnetic coupling system is derived as follows. By applying  $\mathbf{E}_{eff} \cdot$  to Eq. (5d) and  $\mathbf{H}_{eff} \cdot$  to Eq. (5c), we have

$$-\varepsilon \mathbf{E}_{eff} \cdot \frac{\partial}{\partial t} \mathbf{E}_{eff} - \mu \mathbf{H}_{eff} \cdot \frac{\partial}{\partial t} \mathbf{H}_{eff} = -\mathbf{E}_{eff} \cdot (\nabla \times \mathbf{H}_{eff} - \mathbf{J}) + \mathbf{H}_{eff} \cdot (\nabla \times \mathbf{E}_{eff}), \quad (9)$$

which becomes

$$-\frac{\partial}{\partial t}u_{eff} - \nabla \cdot \mathbf{S}_{eff} = \mathbf{E}_{eff} \cdot \mathbf{J} \quad (10)$$

where  $\mathbf{S}_{eff}$  is the effective local poynting vector, representing the energy per unit time, per unit area transported by the fields

$$\mathbf{S}_{eff} = \mathbf{E}_{eff} \times \mathbf{H}_{eff} \quad (11)$$

and  $u_{eff}$  is the effective energy volume density of electromagnetic field, which can be given by

$$u_{eff} = \frac{1}{2}(\varepsilon E_{eff}^2 + \mu H_{eff}^2) \quad (12)$$

Eq. (10) is identical to the conservation of energy for an electromagnetic system except that  $\mathbf{E}$  and  $\mathbf{H}$  are replaced by  $\mathbf{E}_{eff}$  and  $\mathbf{H}_{eff}$ , respectively. Therefore, the decrease of the internal electromagnetic field energy as represented by the effective fields within a volume plus the rate of electromagnetic wave energy radiated out of the volume surface is the rate of energy done by the field on the external free current and the free charges, plus the media spatial motion induced changes in electromagnetic energy density. The effective fields include the energy contributed by the accelerated motion of the medium. Thus, *the contribution made by media movement can be regarded as a “source” for producing electromagnetic waves, the subsequent interaction of which with the medium system satisfy the standard Maxwell’s equations.* This is because the medium motion would inevitably produce Lorentz force, which will affect the electromagnetism in the region. This phenomenon was first noticed as the “anti-flux” example as pointed out by Feynman [15].

### 3.3 Vector potential solutions

We now use the vector potential for solving the equations. The vector potential  $\mathbf{A}$  and  $\varphi$  are as follows:

$$\mathbf{H}_{eff} = \frac{1}{\mu} \nabla \times \mathbf{A} \quad (13a)$$

and a new scalar electric potential  $\varphi$  for electrostatics,

$$\mathbf{E}_{eff} = -\nabla\varphi - \frac{\partial}{\partial t}\mathbf{A} \quad (13b)$$

Eqs. (13a-b) into Eqs. (5a-d), we have,

$$\nabla^2 \mathbf{A} - \varepsilon\mu \frac{\partial^2}{\partial t^2} \mathbf{A} = -\mu\mathbf{J} \quad (14a)$$

$$\nabla^2 \varphi - \varepsilon\mu \frac{\partial^2}{\partial t^2} \varphi = -\frac{\rho}{\varepsilon} \quad (14b)$$

and the Lorentz gauge must be satisfied:

$$\nabla \cdot \mathbf{A} + \varepsilon \mu \frac{\partial}{\partial t} \varphi = 0 \quad (14c)$$

These are nonhomogeneous wave equations for vector potential  $\mathbf{A}$  and  $\varphi$ , which are non-linear differential equations, the total solutions of which may have to be solved numerically, and the electric and magnetic fields derived must satisfy the boundary conditions as defined in Eqs. (7a-d).

Using the Green's function theory, converting Eq. (14a-b) into integral equations, the corresponding special solutions are:

$$\mathbf{A}_s = \frac{\mu}{4\pi} \iiint \frac{1}{|\mathbf{r}-\mathbf{r}'|} \mathbf{J}(\mathbf{r}', t') d\mathbf{r}', \quad (15a)$$

$$\varphi_s = \frac{1}{4\pi\varepsilon} \iiint \frac{1}{|\mathbf{r}-\mathbf{r}'|} [\rho(\mathbf{r}', t')] d\mathbf{r}', \quad (15b)$$

where the time  $t'$  is the retarded time,  $t' = t - |\mathbf{r} - \mathbf{r}'|/c$ , and the speed of the wave if  $c = 1/\sqrt{\mu\varepsilon}$ . The homogenous solutions are given by:

$$\mathbf{A}_h = \frac{1}{2\pi} \int_{-\infty}^{\infty} d\omega [\boldsymbol{\alpha}(\omega) \exp(i\mathbf{K} \cdot \mathbf{r} - i\omega t) + \boldsymbol{\beta}(\omega) \exp(-i\mathbf{K} \cdot \mathbf{r} - i\omega t)]. \quad (16a)$$

$$\varphi_h = \frac{1}{2\pi} \int_{-\infty}^{\infty} d\omega [\boldsymbol{\tau}(\omega) \exp(i\mathbf{K} \cdot \mathbf{r} - i\omega t) + \boldsymbol{\xi}(\omega) \exp(-i\mathbf{K} \cdot \mathbf{r} - i\omega t)]. \quad (16b)$$

The wave vectors  $+\mathbf{K}$  and  $-\mathbf{K}$  represent the forward and backscattering waves, with  $K = \omega(\mu\varepsilon)^{1/2}$ . The coefficients  $\boldsymbol{\alpha}(\omega)$ ,  $\boldsymbol{\beta}(\omega)$ ,  $\boldsymbol{\tau}(\omega)$  and  $\boldsymbol{\xi}(\omega)$  are to be determined by boundary conditions.

### 3.4 Expanded 4-D space

We express the format of the MEs-f-MDMS into tensor format. We now use the classical expressions of following quantities for electrodynamics, the anti-symmetric strength tensor of electromagnetic field [8],

$$F^{\alpha\beta} = \xi^\alpha A^\beta - \xi^\beta A^\alpha \quad (17a)$$

$$F_{\alpha\beta} = \xi_\alpha A_\beta - \xi_\beta A_\alpha \quad (17b)$$

where  $\alpha, \beta = (1,2,3,4)$ , and the newly defined operators are

$$\xi^\alpha = \left( \frac{1}{c} \frac{\partial}{\partial t}, -\nabla \right) \quad (18a)$$

$$\xi_\alpha = \left( \frac{1}{c} \frac{\partial}{\partial t}, \nabla \right) \quad (18b)$$

$$A^\alpha = (c\varphi, \mathbf{A}) \quad (18c)$$

$$A_\alpha = (c\varphi, -\mathbf{A}) \quad (18d)$$

One can prove

$$F^{\alpha\beta} = \begin{pmatrix} 0 & -E_{eff,x}/c & -E_{eff,y}/c & -E_{eff,z}/c \\ E_{eff,x}/c & 0 & -B_{eff,z} & B_{eff,y} \\ E_{eff,y}/c & B_{eff,z} & 0 & -B_{eff,x} \\ E_{eff,z}/c & -B_{eff,y} & B_{eff,x} & 0 \end{pmatrix} \quad (19a)$$

$$F_{\alpha\beta} = \begin{pmatrix} 0 & E_{eff,x}/c & E_{eff,y}/c & E_{eff,z}/c \\ -E_{eff,x}/c & 0 & -B_{eff,z} & B_{eff,y} \\ -E_{eff,y}/c & B_{eff,z} & 0 & -B_{eff,x} \\ -E_{eff,z}/c & -B_{eff,y} & B_{eff,x} & 0 \end{pmatrix} \quad (19b)$$

where  $c = c_m = 1/(\mu\epsilon)^{1/2}$ . We can prove:

$$\xi_\alpha F^{\alpha\beta} = \mu J^\beta \quad (20)$$

where  $J^\beta = (c\rho_\alpha, \mathbf{J}_a)$ . This is the Maxwell's equations for a mechano-driven system. Note Eq. (69) is the same as that for the classical MEs except the operator  $\partial_\alpha$  is replace by  $\xi_\alpha$ .

### 3.5 The Lagrangian function

We now derive the Lagrangian  $L$  for the Maxwell's equations for a mechano-driven system.  $\Lambda$  is assumed to be a function of the density of the Lagrangian of the system  $\Lambda(A_\alpha, \xi_\alpha A_\beta)$ . The density of the Lagrangian for the electromagnetic field is given by [16]

$$\Lambda = F^{\alpha\beta} F_{\alpha\beta} + \mu J^\alpha A_\alpha \quad (21)$$

Using the Lagrangian relation:

$$\frac{\partial \Lambda}{\partial A_\beta} - \xi_\alpha \frac{\partial \Lambda}{\partial (\xi_\alpha A_\beta)} = 0 \quad (22)$$

we have the Maxwell's equations for a medium that has only rotation motion:

$$\xi_\alpha F^{\alpha\beta} = \mu J^\beta \quad (23)$$

### 3.6 The special solutions in time space

The corresponding special solutions of Eqs . (14a-b) can be easily received using the method as listed in [17],

$$\mathbf{H}_{effs} = \frac{1}{\mu} \nabla \times \mathbf{A}_s = \frac{1}{4\pi} \nabla \times \iiint \frac{1}{|\mathbf{r}-\mathbf{r}'|} \mathbf{J}(\mathbf{r}', t') d\mathbf{r}'$$



$$= \frac{1}{4\pi} \iiint \nabla \times \left[ \frac{1}{|\mathbf{r}-\mathbf{r}'|} \mathbf{J}(\mathbf{r}', t') \right] d\mathbf{r}' = \frac{1}{4\pi} \iiint \frac{1}{|\mathbf{r}-\mathbf{r}'|} [\nabla' \times \mathbf{J}(\mathbf{r}', t)] |_{t=t'} d\mathbf{r}'. \quad (24a)$$

where we have used the integral by part and an identity  $\nabla \frac{1}{|\mathbf{r}-\mathbf{r}'|} = -\nabla' \frac{1}{|\mathbf{r}-\mathbf{r}'|}$ ;  $[\nabla' \times \mathbf{J}(\mathbf{r}', t)] |_{t=t'}$  means that the operator only apply to  $\mathbf{r}'$  but not to  $t'$ . The effective electric field is:

$$\begin{aligned} \mathbf{E}_{effs} &= -\nabla\phi_s - \frac{\partial}{\partial t} \mathbf{A}_s = -\frac{1}{4\pi\epsilon} \nabla \iiint \frac{1}{|\mathbf{r}-\mathbf{r}'|} \rho(\mathbf{r}', t') d\mathbf{r}' - \frac{\mu}{4\pi} \frac{\partial}{\partial t} \iiint \frac{1}{|\mathbf{r}-\mathbf{r}'|} \mathbf{J}(\mathbf{r}', t') d\mathbf{r}' \\ &= -\frac{1}{4\pi} \iiint \frac{1}{|\mathbf{r}-\mathbf{r}'|} \{ [\nabla' \rho(\mathbf{r}', t)/\epsilon] |_{t=t'} + \mu \frac{\partial}{\partial t} \mathbf{J}(\mathbf{r}', t') \} d\mathbf{r}', \end{aligned} \quad (24b)$$

where we have used  $\frac{\partial}{\partial t} = \frac{\partial}{\partial t'}$ .

The full solutions are:  $\mathbf{E}_{eff} = \mathbf{E}_{effh} + \mathbf{E}_{effs}$  and  $\mathbf{H}_{eff} = \mathbf{H}_{effh} + \mathbf{H}_{effs}$ , which satisfy the boundary conditions, and the coefficients  $\alpha(\omega)$ ,  $\beta(\omega)$ ,  $\tau(\omega)$  and  $\xi(\omega)$  are thus to be determined. Substituting Eqs. (23-24) into Eq. (8a-b), the special solutions of  $\mathbf{E}$  and  $\mathbf{H}$  can be received as:

$$\begin{aligned} \mathbf{E}_s &= -\frac{1}{4\pi} \{ \iiint \frac{1}{|\mathbf{r}-\mathbf{r}'|} \{ \mu \frac{\partial}{\partial t} \mathbf{J}(\mathbf{r}', t') + [\nabla' \rho(\mathbf{r}', t)/\epsilon] |_{t=t'} \} d\mathbf{r}' + \mu \mathbf{v}_r \times \iiint \frac{1}{|\mathbf{r}-\mathbf{r}'|} [\nabla' \times \mathbf{J}(\mathbf{r}', t)] |_{t=t'} d\mathbf{r}' \\ &\quad - \mu\epsilon \mathbf{v}_r [\mathbf{v}_r \cdot \iiint \frac{1}{|\mathbf{r}-\mathbf{r}'|} \{ \mu \frac{\partial}{\partial t} \mathbf{J}(\mathbf{r}', t') + [\nabla' \rho(\mathbf{r}', t)/\epsilon] |_{t=t'} \} d\mathbf{r}' \} \}, \end{aligned} \quad (25a)$$

$$\begin{aligned} \mathbf{H}_s &= \frac{1}{4\pi} \iiint \frac{1}{|\mathbf{r}-\mathbf{r}'|} [\nabla' \times \mathbf{J}(\mathbf{r}', t)] |_{t=t'} d\mathbf{r}' - \frac{\epsilon}{4\pi} \mathbf{v}_r \times \iiint \frac{1}{|\mathbf{r}-\mathbf{r}'|} \{ \mu \frac{\partial}{\partial t} \mathbf{J}(\mathbf{r}', t') + [\nabla' \rho(\mathbf{r}', t)/\epsilon] |_{t=t'} \} d\mathbf{r}' \\ &\quad - \frac{\mu\epsilon}{4\pi} \mathbf{v}_r \{ \mathbf{v}_r \cdot \iiint \frac{1}{|\mathbf{r}-\mathbf{r}'|} [\nabla' \times \mathbf{J}(\mathbf{r}', t)] |_{t=t'} \} d\mathbf{r}'. \end{aligned} \quad (25b)$$

Eqs. (25a-b) are the same as those received previously using a different method [13].

### 3.7 The special solutions in frequency space

In general, the dielectric permittivity is frequency dependent, so that the dispersion relationship is complex. To include the frequency in the entire theory, we use the Fourier transform and inverse Fourier transform in time and frequency space as defined by:

$$\mathbf{a}(\mathbf{r}, \omega) = \int_{-\infty}^{\infty} dt e^{i\omega t} \mathbf{a}(\mathbf{r}, t), \quad (26a)$$

$$\mathbf{a}(\mathbf{r}, t) = \frac{1}{2\pi} \int_{-\infty}^{\infty} d\omega e^{-i\omega t} \mathbf{a}(\mathbf{r}, \omega). \quad (26b)$$

Take a Fourier transform of Eqs. (5a-d), we have:

$$\epsilon(\omega) \nabla \cdot \mathbf{E}_{eff}(\mathbf{r}, \omega) = \rho(\mathbf{r}, \omega), \quad (27a)$$

$$\mu(\omega) \nabla \cdot \mathbf{H}_{eff}(\mathbf{r}, \omega) = 0, \quad (27b)$$

$$\nabla \times \mathbf{E}_{eff}(\mathbf{r}, \omega) \approx i\omega \mu(\omega) \mathbf{H}_{effs}(\mathbf{r}, \omega), \quad (27c)$$

$$\nabla \times \mathbf{H}_{eff}(\mathbf{r}, \omega) \approx \mathbf{J}_t(\mathbf{r}, \omega) - i\omega\varepsilon(\omega)\mathbf{E}_{eff}(\mathbf{r}, \omega). \quad (27d)$$

where the effective fields are defined as:

$$\mathbf{E}_{eff}(\mathbf{r}, \omega) = \mathbf{E}(\mathbf{r}, \omega) + \mu(\omega) \mathbf{v}_r(\mathbf{r}, \omega) \times * \mathbf{H}(\mathbf{r}, \omega), \quad (28a)$$

$$\mathbf{H}_{eff}(\mathbf{r}, \omega) = \mathbf{H}(\mathbf{r}, \omega) - \varepsilon(\omega) \mathbf{v}_r(\mathbf{r}, \omega) \times * \mathbf{E}(\mathbf{r}, \omega). \quad (28b)$$

where the calculations of  $\cdot$  and  $\times$  are for  $\mathbf{r}$ , and  $*$  is the convolution calculation with respect to  $\omega$  as defined in following:

$$\int_{-\infty}^{\infty} dt e^{i\omega t} \mathbf{a}(\mathbf{r}, t) \times \mathbf{b}(\mathbf{r}, t) = \int_{-\infty}^{\infty} \mathbf{a}(\mathbf{r}, \omega - \omega') \times \mathbf{b}(\mathbf{r}, \omega') d\omega' \equiv \mathbf{a}(\mathbf{r}, \omega) \times * \mathbf{b}(\mathbf{r}, \omega). \quad (29a)$$

The convolution is to the frequency, and the curl is to the space  $\mathbf{r}$ . Similarly, we also define for dot product

$$\int_{-\infty}^{\infty} dt e^{i\omega t} \mathbf{a}(\mathbf{r}, t) \cdot \mathbf{b}(\mathbf{r}, t) = \int_{-\infty}^{\infty} \mathbf{a}(\mathbf{r}, \omega - \omega') \cdot \mathbf{b}(\mathbf{r}, \omega') d\omega' \equiv \mathbf{a}(\mathbf{r}, \omega) \cdot * \mathbf{b}(\mathbf{r}, \omega). \quad (29b)$$

The corresponding boundary conditions are:

$$[\varepsilon_a(\omega)\mathbf{E}_{eff,a}(\mathbf{r}, \omega) - \varepsilon_b(\omega)\mathbf{E}_{eff,b}(\mathbf{r}, \omega)] \cdot * \mathbf{n}(\mathbf{r}, \omega) = \sigma \quad (30a)$$

$$[\mu_a(\omega)\mathbf{H}_{eff,a}(\mathbf{r}, \omega) - \mu_b(\omega)\mathbf{H}_{eff,b}(\mathbf{r}, \omega)] \cdot * \mathbf{n}(\mathbf{r}, \omega) = 0 \quad (30b)$$

$$\mathbf{n}(\mathbf{r}, \omega) \times * [\mathbf{E}_{eff,a}(\mathbf{r}, \omega) - \mathbf{E}_{eff,b}(\mathbf{r}, \omega)] \approx 0 \quad (30c)$$

$$\mathbf{n}(\mathbf{r}, \omega) \times * [\mathbf{H}_{eff,a}(\mathbf{r}, \omega) - \mathbf{H}_{eff,b}(\mathbf{r}, \omega)] \approx \mathbf{K}_s(\mathbf{r}, \omega) + \sigma(\mathbf{r}, \omega) * \mathbf{v}_s(\mathbf{r}, \omega) \quad (30d)$$

We now define the vector potential  $\mathbf{A}$  and  $\varphi$  as follows:

$$\mathbf{H}_{eff}(\mathbf{r}, \omega) = \frac{1}{\mu(\omega)} \nabla \times \mathbf{A}(\mathbf{r}, \omega) \quad (31a)$$

and a new scalar electric potential  $\varphi$  for electrostatics, we define

$$\mathbf{E}_{eff}(\mathbf{r}, \omega) = -\nabla\varphi(\mathbf{r}, \omega) + i\omega\mathbf{A}(\mathbf{r}, \omega) \quad (31b)$$

Eqs. (31a,b) into Eqs. (27a-d), we have,

$$\nabla^2 \mathbf{A}(\mathbf{r}, \omega) + \omega^2 \varepsilon(\omega) \mu(\omega) \mathbf{A}(\mathbf{r}, \omega) = -\mu(\omega) \mathbf{J}(\mathbf{r}, \omega) \quad (32a)$$

$$\nabla^2 \varphi(\mathbf{r}, \omega) + \omega^2 \varepsilon(\omega) \mu(\omega) \varphi(\mathbf{r}, \omega) = -\frac{\rho(\mathbf{r}, \omega)}{\varepsilon(\omega)} \quad (32b)$$

and the Lorentz gauge must be satisfied:

$$\nabla \cdot \mathbf{A}(\mathbf{r}, \omega) - i\omega\varepsilon(\omega)\mu(\omega)\varphi(\mathbf{r}, \omega) = 0 \quad (32c)$$

These are Helmholtz equations for vector potential  $\mathbf{A}$  and  $\varphi$ , which are non-linear differential equations, and the special solutions are given by [17]:

$$\mathbf{A}_s(\mathbf{r}, \omega) = \frac{\mu(\omega)}{4\pi} \iiint \frac{\exp[i\omega\sqrt{\mu\varepsilon}|\mathbf{r}-\mathbf{r}'|]}{|\mathbf{r}-\mathbf{r}'|} \mathbf{J}(\mathbf{r}', \omega) d\mathbf{r}', \quad (33a)$$

$$\varphi_s(\mathbf{r}, \omega) = \frac{1}{4\pi\varepsilon\omega} \iiint \frac{\exp[i\omega\sqrt{\mu\varepsilon}|\mathbf{r}-\mathbf{r}'|]}{|\mathbf{r}-\mathbf{r}'|} \rho(\mathbf{r}', \omega) d\mathbf{r}'. \quad (33b)$$

The homogeneous solutions for the Helmholtz equations are:

$$\mathbf{A}_h(\mathbf{r}, \omega) = \boldsymbol{\alpha} \exp(i\mathbf{K}\cdot\mathbf{r}) + \boldsymbol{\beta} \exp(-i\mathbf{K}\cdot\mathbf{r}). \quad (34a)$$

$$\varphi_h(\mathbf{r}, \omega) = \boldsymbol{\tau} \exp(i\mathbf{K}\cdot\mathbf{r}) + \boldsymbol{\xi} \exp(-i\mathbf{K}\cdot\mathbf{r}). \quad (34b)$$

The special solutions for the effective electric field and magnetic fields are given by:

$$\begin{aligned} \mathbf{E}_{effs}(\mathbf{r}, \omega) &= -\nabla\varphi_s(\mathbf{r}, \omega) + i\omega\mathbf{A}_s(\mathbf{r}, \omega) \\ &= \frac{1}{4\pi} \iiint \frac{\exp[i\omega\sqrt{\mu\varepsilon}|\mathbf{r}-\mathbf{r}'|]}{|\mathbf{r}-\mathbf{r}'|} [i\omega\mu(\omega)\mathbf{J}(\mathbf{r}', \omega) - \nabla'\rho(\mathbf{r}', \omega)/\varepsilon(\omega)] d\mathbf{r}', \end{aligned} \quad (35a)$$

$$\begin{aligned} \mathbf{H}_{effs}(\mathbf{r}, \omega) &= \frac{1}{\mu(\omega)} \nabla \times \mathbf{A}_s(\mathbf{r}, \omega) \\ &= \frac{1}{4\pi} \iiint \frac{\exp[i\omega\sqrt{\mu\varepsilon}|\mathbf{r}-\mathbf{r}'|]}{|\mathbf{r}-\mathbf{r}'|} [\nabla' \times \mathbf{J}(\mathbf{r}', \omega)] d\mathbf{r}'. \end{aligned} \quad (35b)$$

The total solution must satisfy the boundary conditions. Finally, the corresponding electric and magnetic fields may not be easily derived analytically from Eq. (8a-b), we can approximately have

$$\mathbf{E}(\mathbf{r}, \omega) \approx [\mathbf{E}_{eff}(\mathbf{r}, \omega) - \mu\mathbf{v}_r(\mathbf{r}, \omega) \times * \mathbf{H}_{eff}(\mathbf{r}, \omega) - \mu\varepsilon\mathbf{v}_r * (\mathbf{v}_r \cdot * \mathbf{E}_{eff}(\mathbf{r}, \omega))], \quad (36a)$$

$$\mathbf{H}(\mathbf{r}, \omega) \approx [\mathbf{H}_{eff}(\mathbf{r}, \omega) + \varepsilon\mathbf{v}_r(\mathbf{r}, \omega) \times * \mathbf{E}_{eff}(\mathbf{r}, \omega) - \mu\varepsilon\mathbf{v}_r(\mathbf{r}, \omega) * (\mathbf{v}_r(\mathbf{r}, \omega) \cdot * \mathbf{H}_{eff}(\mathbf{r}, \omega))] \quad (36b)$$

## 4. Applications

### 4.1 About classical treatment of electromagnetism of a rotating medium

We now discuss about the limitations in classical treatment of the electromagnetic behavior of a rotating medium, such as a dielectric object as shown in Fig. 2. The motion of the surface charges as driven by the rotating object is taken as a current density  $\mathbf{J} = \rho\mathbf{v}_r$  in theoretical calculation, so the electromagnetic fields in space are governed by

$$\varepsilon\nabla \cdot \mathbf{E} = \rho \quad (37a)$$

$$\mu\nabla \cdot \mathbf{H} = 0 \quad (37b)$$

$$\nabla \times \mathbf{E} \approx -\mu\frac{\partial}{\partial t}\mathbf{H} \quad (37c)$$

$$\nabla \times \mathbf{H} \approx \rho\mathbf{v}_r + \varepsilon\frac{\partial}{\partial t}\mathbf{E} \quad (37d)$$

This treatment appears reasonable and straight forward, but it ignores the contribution made by the Lorentz force contributed by the rotation medium, for example.

Now let's examine this case from the MEs-f-MDMS. From Eq. (5c), we have

$$\begin{aligned}
\nabla \times \mathbf{H} &\approx \mathbf{J} + \varepsilon \frac{\partial}{\partial t} (\mathbf{E} + \mu \mathbf{v}_r \times \mathbf{H}) + \varepsilon \nabla \times (\mathbf{v}_r \times \mathbf{E}) \\
&= \mathbf{J} + \varepsilon \frac{\partial}{\partial t} \mathbf{E} + \varepsilon \mu \frac{\partial}{\partial t} (\mathbf{v}_r \times \mathbf{H}) + \varepsilon [\mathbf{v}_r (\nabla \cdot \mathbf{E}) - \mathbf{E} (\nabla \cdot \mathbf{v}_r) + (\mathbf{E} \cdot \nabla) \mathbf{v}_r - (\mathbf{v}_r \cdot \nabla) \mathbf{E}] \\
&\approx \mathbf{J} + \varepsilon \frac{\partial}{\partial t} \mathbf{E} + \rho \mathbf{v}_r + \varepsilon \mu \frac{\partial}{\partial t} (\mathbf{v}_r \times \mathbf{H}) + \varepsilon [(\mathbf{E} \cdot \nabla) \mathbf{v}_r - \mathbf{E} (\nabla \cdot \mathbf{v}_r) - (\mathbf{v}_r \cdot \nabla) \mathbf{E}].
\end{aligned} \tag{38}$$

The first two terms are the standard terms in classical Maxwell's equations for stationary medium. The additional currents contributed owing to the motion of the medium are:

$$\mathbf{J}_m = \rho \mathbf{v}_r + \varepsilon \mu \frac{\partial}{\partial t} (\mathbf{v}_r \times \mathbf{H}) + \varepsilon [(\mathbf{E} \cdot \nabla) \mathbf{v}_r - \mathbf{E} (\nabla \cdot \mathbf{v}_r) - (\mathbf{v}_r \cdot \nabla) \mathbf{E}]. \tag{39}$$

Now we can discuss about the relative magnitude of  $\rho \mathbf{v}_r$  with respect to last term  $\varepsilon |(\mathbf{v}_r \cdot \nabla) \mathbf{E}| / \rho \mathbf{v}_r \sim \varepsilon |v_r \frac{\partial E}{\partial x}| / \rho \mathbf{v}_r \sim 1$ , the same order. In classical approach, the approach for treating the electrodynamics is to treat the rotating medium as an effective current described by  $\rho \mathbf{v}_r$ , but such a treatment drops out the contribution made by the terms that result from the magnetic to electric induction as described by terms such as  $\{\varepsilon \mu \frac{\partial}{\partial t} (\mathbf{v}_r \times \mathbf{H}) + \varepsilon [(\mathbf{E} \cdot \nabla) \mathbf{v}_r - (\mathbf{v}_r \cdot \nabla) \mathbf{E}]\}$ , which are of the same orders as that from  $\rho \mathbf{v}_r$ ! This means that the treatment of cases such as mechanical antenna by Eqs. (37a-d) in classical approach misses several important contributions, and the full theory for MEs-f-MDMS (Eqs. (5a-d) has to be used.

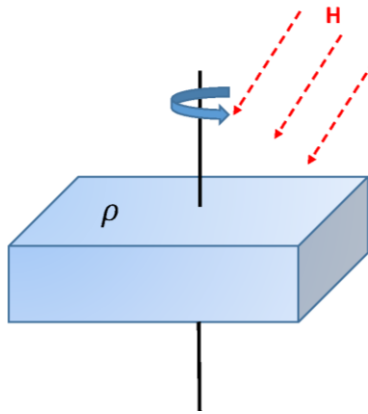


Fig. 2. Schematic diagram showing a rotating medium that has a shape and a non-uniform surface charge density.

Furthermore, we propose a possible explanation for why cell phone signals on a fast-moving train are often weaker than those on the ground. Objects such as trees and buildings on Earth accumulate surface charges due to contact electrification with flowing air. When a train moves in the  $x$ -direction, a relative backward motion of these objects induces a current in the  $-x$  direction. The effect of these charged surfaces is equivalent to introducing a current  $\mathbf{J}_m = \rho \mathbf{v}_r$ , which may appear as a pulse as the objects move away from the observer. Since the size and shape of the objects vary as the train moves forward, the induced current also varies. This time-dependent current in the environment can generate low-frequency noise, which may interfere with the audio system. Additionally, such currents produce electromagnetic radiation across a broad spectrum, likely contributing to environmental noise that degrades the quality of the received signals.

#### 4.2 Quantifying the output of triboelectric nanogenerator

Triboelectric nanogenerator (TENG) is to utilize the triboelectric effect and electrostatic induction effect for converting mechanical energy into electric power [18]. The surface charges are generated by triboelectric effect, the relative movement of the dielectric media results in current flow between the electrodes attached to the dielectric media. As for TENG, inside the dielectric medium that is moving, as schematically shown in Fig. 3, from Eq. (38), the motion induced displacement current density is:

$$\mathbf{J}_m = \rho \mathbf{v}_r + \varepsilon \mu \frac{\partial}{\partial t} (\mathbf{v}_r \times \mathbf{H}) + \varepsilon [(\mathbf{E} \cdot \nabla) \mathbf{v}_r - \mathbf{E} (\nabla \cdot \mathbf{v}_r) - (\mathbf{v}_r \cdot \nabla) \mathbf{E}], \quad (40)$$

where the first term is the current due to the motion of the charged surfaces, and the rest of the terms are produced due to the fields generated owing to the motion of the medium. The total current observed in TENG is an integration of the  $\mathbf{J}_m$  over the surface of the electrode, such as A electrode as shown in Fig. 3:

$$I = \int_{\text{electrode}} \mathbf{J}_m \cdot d\mathbf{s} \quad (41)$$

The electromotive force between the two electrodes A and B is given by:

$$\xi_{\text{EMF}} = \int_{\text{inside}} (\mathbf{E} + \mu \mathbf{v}_r \times \mathbf{H}) \cdot d\mathbf{L} + \int_{\text{outside}} \mathbf{E} \cdot d\mathbf{L} \quad (42)$$

where the first integral is along the circuit inside the dielectric media, and the second term is along the circuit in free-space. If an external load  $R$  is connected, we have  $\xi_{\text{EMF}} = IR$ .

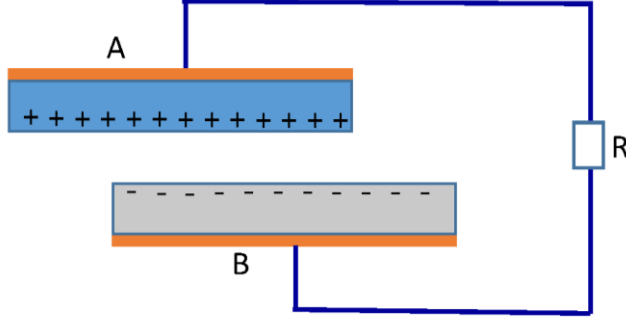


Fig. 3. Schematic diagram showing the basic configuration of a triboelectric nanogenerator and the related circuit for power output.

### 4.3 Reflection of a plane wave at a rotating medium interface

As illustrated in Fig. 4, a plane wave is shining at a planar interface between media  $(\varepsilon_1, \mu_1)$  and  $(\varepsilon_2, \mu_2)$ , and the media system is rotating at an angular velocity  $\omega$  around the z axis, and the corresponding angles are indicated. For simplicity, we assume that the two media are semi-infinity, and we consider only a case that the electric field is parallel to the interface, and the corresponding fields are illustrated. We assume there are no space charges and no free-current,  $\rho = 0$  and  $\mathbf{J} = 0$ . The incidence, reflected and transmitted effective fields that satisfy Eqs. (5a-d) are given by:

$$\mathbf{E}_{eff} = \mathbf{E}_{eff0} \exp(i\mathbf{K} \cdot \mathbf{r} + i\omega t), \quad (43a)$$

$$\mathbf{E}'_{eff} = \mathbf{E}'_{eff0} \exp(i\mathbf{K}' \cdot \mathbf{r} + i\omega t), \quad (43b)$$

$$\mathbf{E}''_{eff} = \mathbf{E}''_{eff0} \exp(i\mathbf{K}'' \cdot \mathbf{r} + i\omega t), \quad (43c)$$

$$\mathbf{H}_{eff} = \mathbf{H}_{eff0} \exp(i\mathbf{K} \cdot \mathbf{r} + i\omega t), \quad (43d)$$

$$\mathbf{H}'_{eff} = \mathbf{H}'_{eff0} \exp(i\mathbf{K}' \cdot \mathbf{r} + i\omega t), \quad (43e)$$

$$\mathbf{H}''_{eff} = \mathbf{H}''_{eff0} \exp(i\mathbf{K}'' \cdot \mathbf{r} + i\omega t), \quad (43f)$$

where the wave vectors and the magnitudes of the plane waves are related by following relationships in order to satisfy the Eq. (5a-d) and the associated boundary conditions (Eqs. (7a-b) [19]:

$$K = K' = \omega \sqrt{\mu_1 \varepsilon_1}, \quad K'' = \omega \sqrt{\mu_2 \varepsilon_2}, \quad (44a)$$

$$E_{eff0}/H_{eff0} = \sqrt{\mu_1/\varepsilon_1}, \quad E'_{eff0}/H'_{eff0} = \sqrt{\mu_1/\varepsilon_1}, \quad E''_{eff0}/H''_{eff0} = \sqrt{\mu_2/\varepsilon_2}. \quad (44b)$$

and  $\sin \theta_2 = \frac{c_2}{c_1} \sin \theta_1$ . From boundary conditions given by Eqs. (7c-d)), we have:

$$H_{eff0} \cos \theta_1 - H'_{eff0} \cos \theta_1 = H''_{eff0} \cos \theta_2, \quad (45a)$$

$$E_{eff0} - E'_{eff0} = E''_{eff0}. \quad (45b)$$

From Eqs. (44-45), we can derive:

$$E'_{eff0} = \frac{\eta_{12} \cos \theta_1 - \cos \theta_2}{\eta_{12} \cos \theta_1 + \cos \theta_2} E_{eff0}, \quad (46a)$$

$$H'_{eff0} = \frac{\eta_{12} \cos \theta_1 - \cos \theta_2}{\eta_{12} \cos \theta_1 + \cos \theta_2} H_{eff0}, \quad (46b)$$

$$E''_{eff0} = \frac{2 \eta_{12} \cos \theta_1}{\eta_{12} \cos \theta_1 + \cos \theta_2} E_{eff0}, \quad (46c)$$

$$H''_{eff0} = \frac{2 \cos \theta_1}{\eta_{12} \cos \theta_1 + \cos \theta_2} H_{eff0}, \quad (46d)$$

where  $\eta_{12} = \sqrt{\mu_2 \epsilon_2 / \mu_1 \epsilon_1}$  and  $\theta_1 = \theta_0 + \varpi t$ , with  $c_2 = \frac{1}{\sqrt{\mu_2 \epsilon_2}}$ ,  $c_1 = \frac{1}{\sqrt{\mu_1 \epsilon_1}}$ , and  $\varpi$  the angular velocity of the interface

rotation. From Eqs. (8a-b), we can derive following wave expressions for the electric and magnetic waves:

The incidence waves in the medium 1 are,

$$\mathbf{E} = [1 + \frac{\varpi r}{c_1} \cos(\theta_1 + \varpi t)] E_{eff} \hat{z}, \quad (47a)$$

$$\mathbf{H} \approx [(\cos \theta_1 - \frac{\varpi r}{c_1} \cos \varpi t) \hat{x} - (\sin \theta_1 + \frac{\varpi r}{c_1} \sin \varpi t) \hat{y}] H_{eff}. \quad (47b)$$

Where  $\hat{x}$ ,  $\hat{y}$  and  $\hat{z}$  are the unit vectors along the x-, y- and z-axis, respectively.

The reflected wave in medium 1 are:

$$\mathbf{E}' = \frac{\eta_{12} \cos(\theta_1) - \cos(\theta_2)}{\eta_{12} \cos(\theta_1) + \cos(\theta_2)} (1 - \frac{\varpi r}{c_1} \cos \theta_0) E_{eff} \hat{z}, \quad (48a)$$

$$\mathbf{H}' \approx \frac{\eta_{12} \cos(\theta_1) - \cos(\theta_2)}{\eta_{12} \cos(\theta_1) + \cos(\theta_2)} [(-\cos \theta_1 + \frac{\varpi r}{c_1} \cos \varpi t) \hat{x} + (-\sin \theta_1 + \frac{\varpi r}{c_1} \sin \varpi t) \hat{y}] H_{eff}. \quad (48b)$$

The transmitted wave in medium 2 are:

$$\mathbf{E}'' = \frac{2 \eta_{12} \cos \theta_1}{\eta_{12} \cos \theta_1 + \cos \theta_2} [1 + \frac{\varpi r}{c_2} \cos(\theta_2 + \varpi t)] E_{eff} \hat{z}, \quad (49a)$$

$$\mathbf{H}'' \approx - \frac{2 \cos \theta_1}{\eta_{12} \cos \theta_1 + \cos \theta_2} [(\cos \theta_2 - \frac{\varpi r}{c_2} \sin \varpi t) \hat{x} + (-\sin \theta_2 + \frac{\varpi r}{c_2} \cos \varpi t) \hat{y}] H_{eff}. \quad (49b)$$

We recall that the MWS-f-MDMS were derived for slow moving medium case under an approximation of  $\varpi r \ll c$ , so that the corrections made by the interface rotation to the reflection and refraction of the medium boundary is rather small. In any case, the medium motion can slightly change the amplitudes of the waves. This means that the movement of flying object has very little effect on the reflected wave. If the receiver has enough sensitivity, it should be possible to measure the rotating status of the object, possibly useful for future virtual reality.

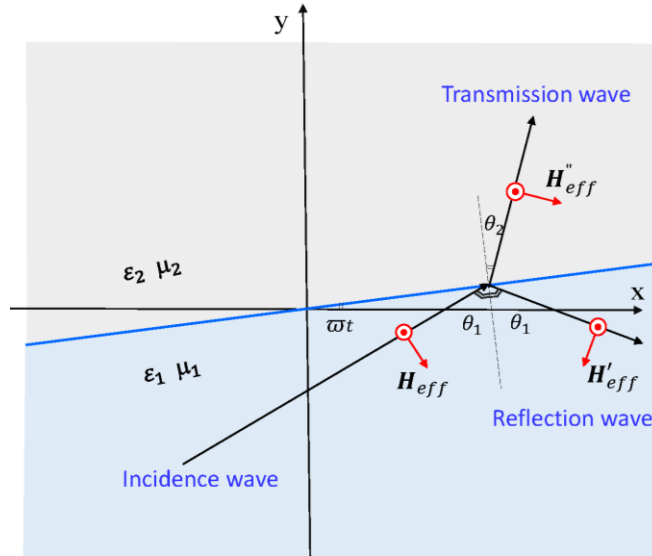


Fig. 4. Schematic diagram showing a plane wave that incidences on an interface between two media that is rotating around the z-axis.

### 5. Extrapolation to a general case including uniform translation motion

We now consider a case in which the medium motion in the Lab frame  $S$  can be described using a uniform translation velocity along a straight line and an accelerated component in  $S'$  frame:  $\mathbf{v}_0 + \mathbf{v}_r(\mathbf{r}, t)$ , as shown in Fig. 5. The moving reference frame  $S'$  with respect to Lab frame  $S$  can be described by a constant velocity  $\mathbf{v}_0$ , which does not have to be a low moving velocity for a general case. In this case, we have to consider relativistic effect due to high moving velocity, and we may need to use relativistic space-time. In the moving reference frame  $S'$ , the accelerated component is a low speed motion with respect to  $S'$ , so that we can approximately use Galilean space-time. Our theoretical derivation can be considered as two steps, as described in follows.

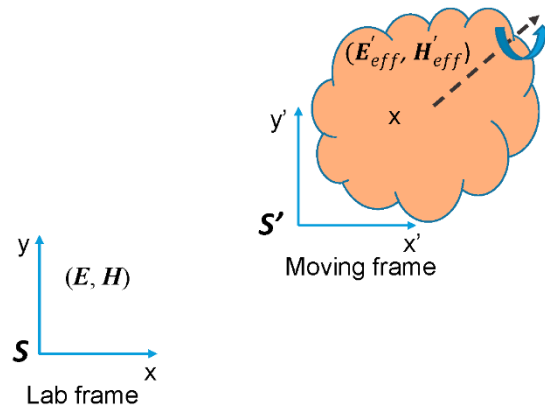




Figure 5. Schematic diagram showing a referene frame  $S'$  that is moving at a constant velocity  $\mathbf{v}_0$  with respect to the Lab frame  $S$ . The rotation of the medium in  $S'$  frame can be treated using the effective field approach, and the fields to be observed in the Lab frame can be derived using the Lorentz transformation.

In the first step, in the  $S'$  reference frame ( $\mathbf{r}'$ ,  $t'$ ), the electromagnetic behavior ( $\mathbf{E}'$ ,  $\mathbf{H}'$ ) of the “rotating” medium can be described using the theory presented in Section 3:

$$\nabla' \cdot \mathbf{D}'_{eff} = \rho \quad (50a)$$

$$\nabla' \cdot \mathbf{B}'_{eff} = 0 \quad (50b)$$

$$\nabla' \times \mathbf{E}'_{eff} \approx -\frac{\partial}{\partial t'} \mathbf{B}'_{eff} \quad (50c)$$

$$\nabla' \times \mathbf{H}'_{eff} \approx \mathbf{J} + \frac{\partial}{\partial t'} \mathbf{D}'_{eff} \quad (50d)$$

where the effective fields are defined by:

$$\mathbf{D}'_{eff} = \varepsilon \mathbf{E}'_{eff}, \quad (51a)$$

$$\mathbf{B}'_{eff} = \mu \mathbf{H}'_{eff}. \quad (51b)$$

$$\mathbf{E}'_{eff} = \mathbf{E}' + \mu \mathbf{v}_r \times \mathbf{H}', \quad (51c)$$

$$\mathbf{H}'_{eff} = \mathbf{H}' - \varepsilon \mathbf{v}_r \times \mathbf{E}'. \quad (51d)$$

The solution of which can be received using the methods described in Sections 3.

In the second step, we can use the Lorentz transformation to derive the relationship between the fields observed in Lab frame  $S$  with that in the moving frame  $S'$ . Since the  $S$  and  $S'$  frames are inertia reference frames, the covariance of the Maxwell's equations is preserved. If this is the case, the fields in the two reference frames can be derived using Lorentz transformation provided the Maxwell's equations are covariant, and the results are given by [14]:

$$\mathbf{E} = \gamma(\mathbf{E}' - \mathbf{v} \times \mathbf{B}') - (\gamma - 1)\mathbf{E}'_{\parallel}, \quad (52a)$$

$$\mathbf{B} = \gamma\left(\mathbf{B}' + \frac{1}{c_0^2} \mathbf{v} \times \mathbf{E}'\right) - (\gamma - 1)\mathbf{B}'_{\parallel}. \quad (52b)$$

$$\mathbf{D} = \gamma\left(\mathbf{D}' - \frac{1}{c_0^2} \mathbf{v} \times \mathbf{H}'\right) - (\gamma - 1)\mathbf{D}'_{\parallel}, \quad (52c)$$

$$\mathbf{H} = \gamma(\mathbf{H}' + \mathbf{v} \times \mathbf{D}') - (\gamma - 1)\mathbf{H}'_{\parallel}. \quad (52d)$$

where  $\mathbf{E}'_{\parallel}$ ,  $\mathbf{B}'_{\parallel}$ ,  $\mathbf{H}'_{\parallel}$  and  $\mathbf{D}'_{\parallel}$  are the components of  $\mathbf{E}'$ ,  $\mathbf{B}'$ ,  $\mathbf{H}'$  and  $\mathbf{D}'$  parallel to the velocity  $\mathbf{v}_0$ , respectively; and  $c_0$  is the speed of light in free-space. This is the result we quoted from standard text book.

Now we may use the relationships given in Eqs. (51a-d) to correlated the effective fields ( $\mathbf{E}'_{eff}, \mathbf{H}'_{eff}$ ) in the moving reference frame with that in the Lab frame ( $\mathbf{E}, \mathbf{H}$ ) based on following discussion. Since the governing equations for  $\mathbf{E}'_{eff}$ , and  $\mathbf{H}'_{eff}$  are the standard Maxwell's equations (see Eqs. (5a-d)), and if the covariance of the Maxwell's equations is still preserved for ( $\mathbf{E}, \mathbf{H}$ ) in Lab frame, we may approximately use the relationship derived based on Lorentz transformation as for electromagnetism in free-space as given in Eqs. (52a-d). By replacing  $\mathbf{E}', \mathbf{B}', \mathbf{H}'$  and  $\mathbf{D}'$  by  $\mathbf{E}'_{eff}, \mathbf{B}'_{eff}, \mathbf{H}'_{eff}$  and  $\mathbf{D}'_{eff}$ , respectively, in Eq. (52a-d), we have:

$$\mathbf{E} = \gamma(\mathbf{E}'_{eff} - \mathbf{v}_0 \times \mathbf{B}'_{eff}) - (\gamma - 1)\mathbf{E}'_{eff,\parallel} = \gamma(\mathbf{E}'_{eff} - \mu \mathbf{v}_0 \times \mathbf{H}'_{eff}) - (\gamma - 1)\mathbf{E}'_{eff,\parallel} \quad (53a)$$

$$\mathbf{B} = \gamma\left(\mathbf{B}'_{eff} + \frac{1}{c_0^2} \mathbf{v}_0 \times \mathbf{E}'_{eff}\right) - (\gamma - 1)\mathbf{B}'_{eff,\parallel} = \gamma\left(\mu \mathbf{H}'_{eff} + \frac{1}{c_0^2} \mathbf{v}_0 \times \mathbf{E}'_{eff}\right) - \mu(\gamma - 1)\mathbf{H}'_{eff,\parallel} \quad (53b)$$

$$\mathbf{D} = \gamma\left(\mathbf{D}'_{eff} - \frac{1}{c_0^2} \mathbf{v}_0 \times \mathbf{H}'_{eff}\right) - (\gamma - 1)\mathbf{D}'_{eff,\parallel} = \gamma\left(\varepsilon \mathbf{E}'_{eff} - \frac{1}{c_0^2} \mathbf{v}_0 \times \mathbf{H}'_{eff}\right) - \varepsilon(\gamma - 1)\mathbf{E}'_{eff,\parallel} \quad (53c)$$

$$\mathbf{H} = \gamma(\mathbf{H}'_{eff} + \mathbf{v}_0 \times \mathbf{D}'_{eff}) - (\gamma - 1)\mathbf{H}'_{eff,\parallel} = \gamma(\mathbf{H}'_{eff} + \varepsilon \mathbf{v}_0 \times \mathbf{E}'_{eff}) - (\gamma - 1)\mathbf{H}'_{eff,\parallel} \quad (53d)$$

where  $\gamma = (1 - v_0^2/c_0^2)^{-1/2}$ . Equations (53a-d) expands the MEs-f-MDMS to include relativistic effect. Equations (53a-d) means that we have expanded the MEs-f-MDMS derived under Galilean space and time to relativistic space and time.

If the moving velocity is much smaller than the speed of light,  $v_0 \ll c_0$ , Eqs. (53a-d) are approximated as:

$$\mathbf{E} \approx \mathbf{E}'_{eff} - \mu \mathbf{v}_0 \times \mathbf{H}'_{eff} \quad (54a)$$

$$\mathbf{B} \approx \mu \mathbf{H}'_{eff} + \frac{1}{c_0^2} \mathbf{v}_0 \times \mathbf{E}'_{eff} \quad (54b)$$

$$\mathbf{D} \approx \varepsilon \mathbf{E}'_{eff} - \frac{1}{c_0^2} \mathbf{v}_0 \times \mathbf{H}'_{eff} \quad (54c)$$

$$\mathbf{H} \approx \mathbf{H}'_{eff} + \varepsilon \mathbf{v}_0 \times \mathbf{E}'_{eff} \quad (54d)$$

It appears that the effective fields are an important approach for dealing with the electromagnetic theory of a moving medium system in general. Equations (54a and d) are equivalent to that given in Eqs. (8a-b) at low moving velocity approximation.

## 6. Experimental observations of the electromagnetism of rotating medium

There are numerous examples reporting about the electromagnetic phenomena in rotating medium system that can not be fully described using the MEs because they were derived under the approximation of stationary media. Here we present a few cases that involves the electromagnetic radiation produced by moving media.

### 6.1 The Röntgen and Eichenwald Experiments

We now consider a simple case in which the electric field is a constant,  $\frac{\partial}{\partial t} \mathbf{D} = 0$ , and there are no external current or charges, Eq. (1d) gives,  $\nabla \times \mathbf{H} \approx \nabla \times (\mathbf{v}_r \times \mathbf{D})$ . This means that a magnetic field  $\mathbf{H} \approx \mathbf{v}_r \times \mathbf{D}$  would be generated if a medium is rotating inside an electric field. The outcomes of the Röntgen and Eichenwald experiments, depicted in Fig. 6 [20]. are typically included in discussions of special relativity. However, we argue that these experiments are unrelated to special relativity due to the extremely low velocities involved. Instead, they are better explained by the electromagnetism of moving objects or media, as described by Eq. (1a-d).

A circular hard rubber disc of thickness  $d$  is mounted on bearings, allowing it to rotate freely about a vertical axis, as illustrated in Fig. 6a. Rigidly attached above and below the disc are metal rings with a radial width  $b$ . Each metal ring is interrupted by a narrow radial slit. The two rings are connected to the terminals of a voltage source, creating a potential difference  $V$  between them. The entire apparatus, including the rubber disc and metal rings, can be set into rotational motion as a single solid unit (as in the Rowland experiment). In this setup, we observe the following charge distributions: true surface charges on the metal plates, given by  $\sigma_1 = \epsilon V/d$ , and surface charges on the hard rubber disc, given by  $\sigma_2 = -(\epsilon - 1)V/d$ . When both the disc and the rings are set into rotation, the upper metal ring carries a convection current  $vb\sigma_1$  along its circumference, where  $v$  is the linear rotational speed of the ring. Simultaneously, the adjacent surface of the hard rubber disc carries a convection current  $vb\sigma_2$ . The total convection current is therefore  $vb(\sigma_1 + \sigma_2) = vbV/d$ . This current corresponds to the second term on the right-hand side of Eq. (1d).

Alternatively, if the metal rings in Fig. 6a are not attached to the rubber disc and only the rubber disc is set into rotation while the metal rings remain stationary (as in the Röntgen experiment), with the circuit connection illustrated in Fig. 6b, the convection current arises solely from the motion of the charges on the surface of the rotating rubber disc, which is  $-vb(\epsilon - 1)V/d$ .

Additionally, the correction to the local magnetic field caused by the motion of a polarized medium is represented by the second term,  $-\nabla \times (\mathbf{v}_r \times \mathbf{D})$ , in Eq. (1d). In the setup depicted in Fig. 6c, a rotating hard-rubber disc is positioned between two stationary and unattached metal rings. The upper ring consists of two semicircular halves, while the lower ring is grounded. The two upper halves are connected to equal but opposite electric potentials,  $+V$  and  $-V$ . A pivoted magnetized needle, free to rotate about a vertical axis, is placed above the disc near the rotation axis to measure the local magnetic field. The convection currents in the two semi-rings flow in opposite directions. Since the polarizations in the regions below the two semi-rings are opposite, a polarization current, represented by the term  $[\nabla \times (\mathbf{v}_r \times \mathbf{D}) + \frac{\partial}{\partial t} \mathbf{D}]$ , flows parallel to the axis of rotation—for example, from point  $a$  to  $b$  (or from  $b$  to  $a'$  on the return path), as indicated in Fig. 6c. This polarization current

ensures the continuity of the convection current in accordance with the conservation of charge. Alternatively, point  $a'$  can be viewed as a charge sink, while point  $a$  acts as a charge source. The conservation of charge is maintained by the presence of the displacement current. Here, the polarization current is part of the displacement current, while the convection current is part of the conduction current.

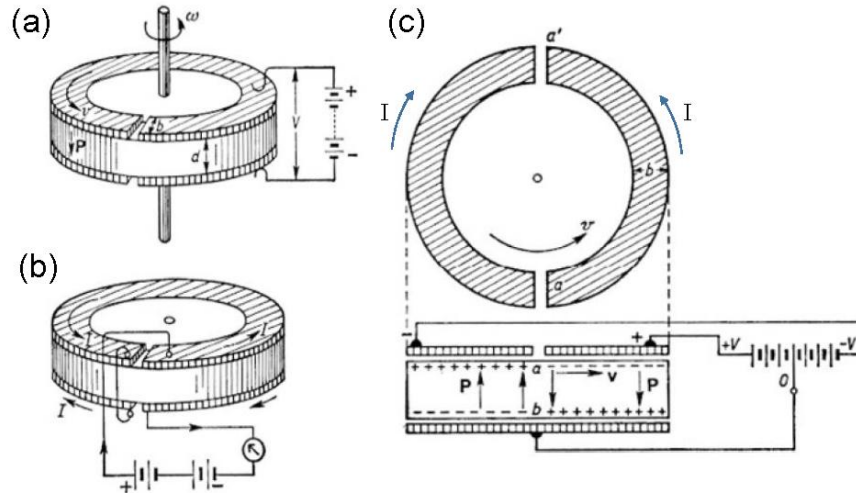


Figure 6. (a) Experiment of Röntgen and Eichenwald. (b) Measurement of the convection current ( $\rho\mathbf{v}$ ) that produces the same magnetic field as in (a). (c) Method of measuring the magnetic field produced by a polarization current represented by  $[\nabla \times (\mathbf{v}_r \times \mathbf{D}) + \frac{\partial \mathbf{D}}{\partial t}]$ . Copyright of [20].

## 6.2 Electromagnetic Radiation from a Rotating Medium Disk in a Constant Magnetic Field

The example of the “anti-flux” provided by Feynman refers to magnetic flux calculated geometrically in circuits with large conductors, where the flux does not satisfy the flux law. Based on this example, we now discuss the electromagnetic radiation generated by an independent metal disk, without any loop, rotating in a constant magnetic field. First, in the experiment, a planetary gear structure was designed to ensure that the geometric center of the rotating metal disk completely coincides with the geometric center of the static magnetic field, as shown in Figure 7a. Under these conditions, the rotation of the metal disk does not alter its own magnetic flux. Additionally, no closed-loop equivalent is formed by connecting the center and edge of the rotating disk, thus avoiding the flux change in an equivalent closed loop that would normally result from a change in magnetic flux [21].

Next, low-frequency electromagnetic wave signals were received using copper coils to couple with the magnetic field. To minimize signal attenuation caused by the copper coil and feed lines, impedance matching was achieved using an LCR meter to ensure maximum power transmission for the electromagnetic wave signals.

Electromagnetic wave signals are highly susceptible to external environmental interference. Therefore, we measured possible sources of electromagnetic interference from three aspects and recorded each signal quantitatively. We recorded the long-time-averaged electromagnetic wave spectrum of signals in the target frequency range (10 Hz - 2 kHz) in the environment, and also measured the electromagnetic wave spectrum signals when the experimental apparatus without the metal disk was operating normally. This signal was taken as the basic background noise, from which we further measured the electromagnetic wave signals generated by the rotating metal disk.

The center frequency of the electromagnetic wave signal generated by the rotating metal disk in the static magnetic field was 805 Hz, with a maximum signal strength of -70 dBm. The overall signal strength was related to the disk's rotational speed, and the bandwidth of the electromagnetic wave signal also increased with the rotational speed (Figure 7b). This experimental result is due to electromagnetic radiation generated by the motion of the medium, which does not align with the predictions of the classical Maxwell equations. On the contrary, this experiment confirms the correctness of the dynamic Maxwell equations. The terms in the equations related to the motion of the medium,  $\nabla \times (\mathbf{v}_r \times \mathbf{B})$  and  $\nabla \times (\mathbf{v}_r \times \mathbf{D})$ , are the sources of the electromagnetic waves. Even in a constant magnetic field, where  $\frac{\partial \mathbf{B}}{\partial t} = 0$ , a corresponding electric field  $\mathbf{E} = -\mathbf{v}_r \times \mathbf{B}$  is generated, and the corresponding magnetic field increment is  $\Delta \mathbf{H} = \mathbf{v}_r \times \mathbf{D}$ . This is why electromagnetic radiation can be observed in the experiment. Due to the high-frequency eddy currents induced in the metal disk, the radiated electromagnetic waves are a superposition of multiple frequencies.

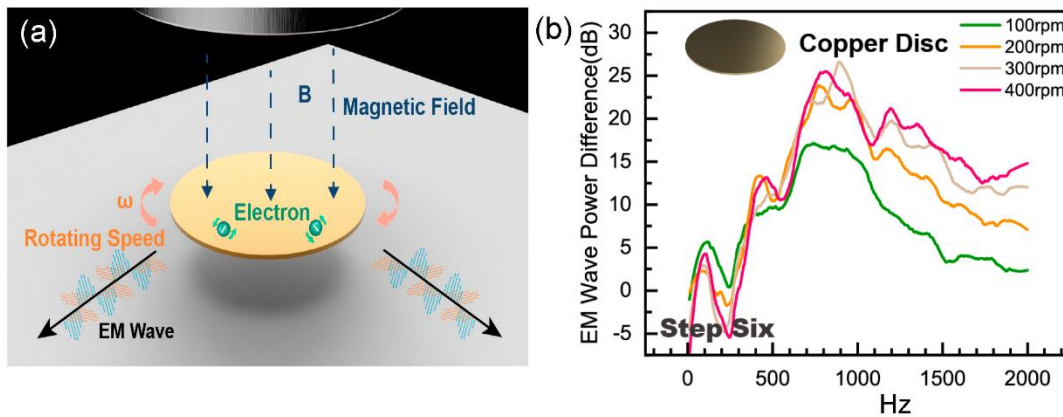


Figure 7. (a) Schematic diagram of the electromagnetic wave experiment based on the dynamic Maxwell equations. (b) Electromagnetic wave signal from a rotating disk under a constant magnetic flux [21].

### 6.3 Underwater Electromagnetic Wave Transmission Triggered by Sound via TENG

To validate the predictions of the dynamic Maxwell equations, we demonstrate an underwater wireless communication method based on the Maxwell's displacement current. Using a microphone-type triboelectric nanogenerator (TENG), sound is converted into electrical signals. This TENG is connected to an emitting electrode that generates a time-varying polarization electric field underwater, and the current can be detected at the receiving electrode at the other end of the water using an electrometer (Figure 8a) [22].

The microphone-type TENG consists of a fluorinated ethylene propylene (FEP) film with a backside-printed conductive ink electrode and an aluminum electrode. The ink electrode is grounded, and the aluminum electrode is connected to the transmitting electrode in the water, operating in a single-electrode mode. Experimental results show that the current signals generated by the TENG have good interference resistance underwater. After passing through a 100-meter-long saline water pipeline, the peak value of the current signal decreases by 66% compared to the original signal, but the waveform of the electrical signal remains undistorted.

Additionally, we demonstrate the application of wireless control for underwater lighting systems. Signals containing voice information (e.g., the words "red" and "green") are transmitted underwater and received by an electrometer, with the current signals shown in Figure 8b. By performing short-time Fourier transform on the signals, a neural network algorithm can distinguish between the words "red" and "green" (Figure 8c). These words are then converted into digital signals to control the on/off state of the light. This method can be applied for real-time voice control of underwater lights (Figure 8d), and the entire underwater communication system powered by TENG is self-sustaining. This work provides an effective communication method for underwater environments, which offers stronger resistance to interference compared to traditional acoustic, optical, and electromagnetic communications, and holds great potential for applications in complex underwater environments.

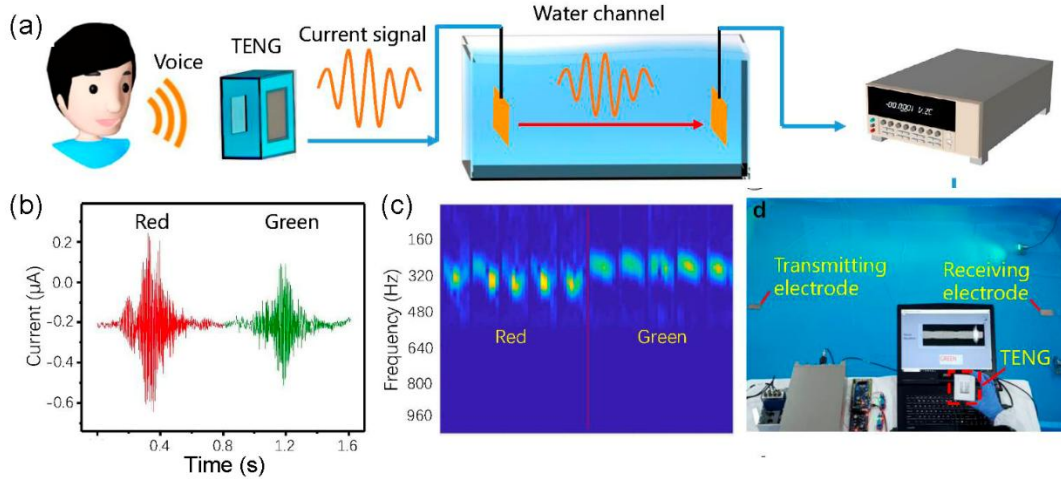


Figure 8. (a) Schematic diagram of converting voice into electrical signals using TENG and achieving underwater wireless communication through Maxwell's displacement current. (b) Received current signals for the words "red" and "green." (c) Short-time Fourier transform of the current signals for "red" and "green." (d) Photo of the experimental setup for wireless voice control [22].

#### 6.4 Wireless Power Transfer Using Displacement Current Generated by TENG

We designed a novel electrode-free triboelectric nanogenerator (TENG) to achieve wireless power transfer by generating Maxwell's displacement current, demonstrating that a moving medium can produce electromagnetic radiation energy [23]. This TENG consists of a polypropylene (PP) disk and a polymethyl methacrylate (PMMA) sector that rotate relative to each other, along with a metal collector. The diameters of the PP disk and PMMA sector are 30 cm and 25 cm, respectively, and both have a thickness of 5 mm. The rotational friction between the PP disk and the PMMA sector generates opposite polarization charges on the friction surfaces. During the rotation, the periodic change in charge distribution causes the spatial displacement field to vary periodically, resulting in a displacement current that depends on the spatial location. This TENG, based on displacement current, converts rotational mechanical energy from the environment into electrical energy and can continuously power portable wearable electronic devices (Figure 9a). When the vertical distance between the metal collector and the PP disk is 3 cm and the rotation speed is 1000 rpm, the open-circuit voltage of the rotating TENG reaches 65 V, and the short-circuit current density reaches  $7 \mu\text{A cm}^{-2}$  (Figures 9b-c). This current density increases proportionally with the rotation speed (Figure 9d), while the voltage change is relatively small. Moreover, experimental results show that the wireless energy transfer distance can reach up to 18 cm. The innovative findings of this work open up new pathways for non-contact wireless power transfer.

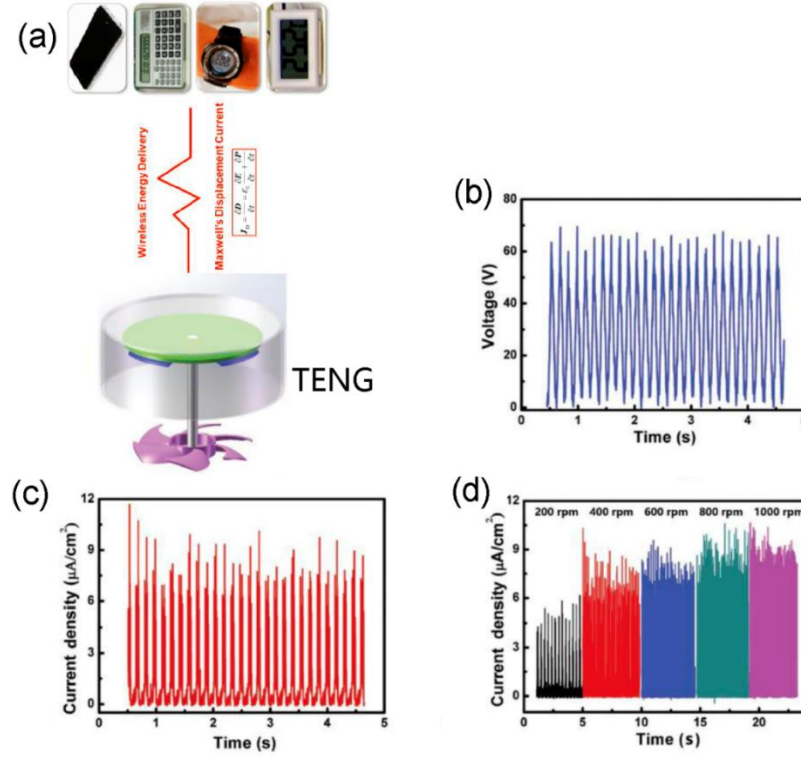


Figure 9. (a) Schematic diagram of an electrode-free rotating TENG achieving wireless energy transfer using Maxwell's displacement current to power portable electronic devices. (b-c) Open-circuit voltage and short-circuit current density of the electrode-free TENG. (d) Relationship between short-circuit current density and rotation speed of the electrode-free TENG [23].

## 7. Summary

In this paper, we have developed the applications of the Maxwell's equations for a motion driven medium system (MEs-f-MDMS) in several cases:

1. For a medium system that is dominated by a rotation type of motion, the MEs-f-MDMS reduce to the standard Maxwell's equations by replacing the electric and magnetic fields by two newly defined effective fields. In such a case, all of the methods for solving the MEs are applicable for solving the MEs-f-MDMS, and the final fields measured can be derived. The newly defined effective fields also satisfy the law of conservation of energy. We conclude that the contribution made by media movement can be regarded as a "source" for producing electromagnetic waves, the subsequent interaction of which with the medium system satisfy the standard Maxwell's equations. This is because the medium motion would inevitably produce Lorentz force, which will affect the electromagnetism in the region.



2. The electromagnetism of a rotation medium system was calculated by treating the medium driven motion of the surface charges as an effective current  $\rho\mathbf{v}_r$  in classical approach. However, such treatment missed the contributions of the currents contributed due to the motion of the medium, which have to be included using the effective field approach. This is necessary in order to explain some of the experimental observations.
3. Furthermore, since the effective fields satisfy the standard MEs, so that their covariance under Lorentz transformation is preserved. The effective field approach can be further expanded to include the case that the system has a uniform translation motion by using the Lorentz transformation as for special relativity. This expands the applications of the MEs-f-MDMS to a case in which the relativistic effect is important.

## References

---

- [1] Minkowski H 1920 *The Principle of Relativity* (University Press)
- [2] Minkowski H 1915 Das Relativitätsprinzip *Ann. Phys.* **352** 927-938
- [3] Pauli W 1958 *Theory of Relativity* (Pergamon)
- [4] Lax L and Nelson D F 1974 Maxwell equations in material form *Physical Rev. B* **13** 1777
- [5] Tai C T 1964 A study of electrodynamics of moving media *Proc. IEEE* **52** 685
- [6] Erden F and Tretyakov O A 2021 A Novel Simple Format of Maxwell's Equations in SI Units *IEEE* **9** 8827
- [7] Wang Z L 2022 The expanded Maxwell's equations for a mechano-driven media system that moves with acceleration *Intern. J. of Modern Physics* **37** 2350159
- [8] Wang Z L, Shao J. Recent progress on Maxwell's equations for a mechano-driven medium system for multi-moving-objects/media, *Electromagnetic Science*. 2023, 2: 0020171.
- [9] Wang Z L 2024 The Maxwell's equations for a mechano-driven media system (MEs-f-MDMS) *Advances in Physics: X* **9** 2354767
- [10] Li E-P, Wang Z L, *New Advances in Maxwell's Equations and Applications*, Springer Nature (2024), Chapter 7.
- [11] Le Bellac M and Lévy-Leblond J M 1973 Galilean electromagnetism. *Nuovo Cim B* **14** 217-234
- [12] Levy-Leblond J M 1965 Une nouvelle limite non-relativiste du groupe de Poincare Section A: Physique Theorique *Ann. Inst. Henri Poincare*. III. **3** 1-12
- [13] Wang Z L 2024 General solutions of the Maxwell's equations for a mechano-driven media system (MEs-f-MDMS) *J. of Physics Communications* **8** 115004
- [14] Rousseaux G 2013 Forty years of Galilean Eelectromagnetism (1973–2013) *Eur Phys J Plus* **128** 1-14
- [15] Feynman R P 2011 *The Feynman Lectures on Physics Vol. II: Mainly Electromagnetism and Matter*. New Millennium Ed. Edition
- [16] [https://en.wikipedia.org/wiki/Covariant\\_formulation\\_of\\_classical\\_electromagnetism](https://en.wikipedia.org/wiki/Covariant_formulation_of_classical_electromagnetism)
- [17] Jackson J D 1999 *Classical Electrodynamics*. 3rd ed. Section 6.4 (John Wiley & Sons)
- [18] Wang Z L 2021 From contact electrification to triboelectric nanogenerators (Review) *Report on Progress in Physics* **84** 096502
- [19] Zangwill A 2013 *Modern Electrodynamics* (Cambridge University Press)
- [20] Becker R 1964 *Electromagnetic fields and interactions Chapter D IV* (Dover Publications)
- [21] Shang Y, Cao L N Y, Su E, Tang W and Wang Z L Dynamics of Electromagnetic Waves Generation by a Rotating Dielectric Disc in a Constant Magnetic Field – A Revisit to Feynman's "Anti-flux"

- [22] Zhao H, Xu M, Shu M, An J, Ding W, Liu X, Wang S, Zhao C, Yu H, Wang H, Wang C, Fu X, Pan X, Xie G 2022 Underwater wireless communication via TENG-generated Maxwell's displacement current, *Nat. Commun.* **13** 3325
- [23] Cao X, Zhang M, Huang J R, Jiang T, Zou J D and Wang N 2018 Inductor-Free Wireless Energy Delivery via Maxwell's Displacement Current from an Electrodeless Triboelectric Nanogenerator *Adv. Mater.* **30** 1704077